NEUROSCIENCE

Social isolation–related depression accelerates ethanol intake via microglia-derived neuroinflammation

Jin-Seok Lee[1], Sung-Bae Lee[1], Dong-Woon Kim[2], Nara Shin[2], Seon-Ju Jeong[3], Chae-Ha Yang[3], Chang-Gue Son[1]*

Social isolation is common in modern society and is a contributor to depressive disorders. People with depression are highly vulnerable to alcohol use, and abusive alcohol consumption is a well-known obstacle to treating depressive disorders. Using a mouse model involving isolation stress (IS) and/or ethanol intake, we investigated the mutual influence between IS-derived depressive and ethanol-seeking behaviors along with the underlying mechanisms. IS increased ethanol craving, which robustly exacerbated depressive-like behaviors. Ethanol intake activated the mesolimbic dopaminergic system, as evidenced by dopamine/tyrosine hydroxylase double-positive signals in the ventral tegmental area and c-Fos activity in the nucleus accumbens. IS-induced ethanol intake also reduced serotonergic activity, via microglial hyperactivation in raphe nuclei, that was notably attenuated by a microglial inhibitor (minocycline). Our study demonstrated that microglial activation is a key mediator in the vicious cycle between depression and alcohol consumption. We also propose that dopaminergic reward might be involved in this pathogenicity.

INTRODUCTION

Depression is the most common neuropsychiatric disorder, with a prevalence of 350 million individuals worldwide (*1*). Patients with depressive disorder had a 20- to 40-fold higher risk of suicidality than healthy individuals (*2*). Recently, our society has emphasized individualism, and these social changes have led to an increase in the prevalence of depressive disorder (*3*, *4*). Social withdrawal is a more potent cause of depression than work-derived stress (*5*). People who live an involuntary solitary life tend to have more suicidal ideation than others in the general population (*6*). Several studies have reported that the recent COVID-19 pandemic–related social isolation has increased the prevalence of depression and anxiety (*7*, *8*).

A plausible mechanism for depression is known as the serotonin depletion hypothesis (*9*). Thus, medications targeting the serotonergic system, such as selective serotonin reuptake inhibitors (SSRIs), are the most frequently prescribed medications to patients with depressive disorders (*10*). However, these antidepressants have limitations such as a low response rate (approximately 47%), a high remission rate (approximately 28%), and a high risk of relapse following drug withdrawal (approximately 62% with fluoxetine) (*11*–*13*). Recently, neuroinflammation has been proposed as one pathophysiologic basis of depression and is considered a promising therapeutic target (*14*, *15*).

On the other hand, to escape from sadness and melancholy, individuals with depression are prone to addiction, especially excessive alcohol use (*16*). Clinical reports have shown that approximately 40.3% of patients with major depressive disorder (MDD) have alcohol use disorder (AUD) (*17*), and conversely, 63.8% of those with AUD have a high prevalence of major depression (*18*). Alcohol use magnifies suicide risk and leads to serotonergic hypoactivity in patients with depressive disorder (*19*). As expected, uncontrolled alcohol use is known to promote the pathological progression and to hinder the treatment of depression (*20*, *21*). Previously, the transcriptome analysis showed increased levels of translocator protein in activated microglia in the human alcoholic brain as a neuroinflammatory feature (*22*). However, the pathological mechanisms of the negative mutual interaction between depression and alcohol consumption remain unclear. Here, we used a mouse model involving social isolation stress (IS) and/or voluntary ethanol intake and explored the mechanisms underlying the interaction between IS-induced depression and ethanol-seeking behaviors.

RESULTS

Voluntary ethanol intake during IS

IS increased voluntary ethanol intake (but not tap water intake) approximately 2.0- to 2.5-fold over the course of 28 days compared to that in the control group ($P < 0.05$ and $P < 0.01$; Fig. 1, A and B). This phenomenon tended to be similar in female mice (fig. S2D). Meanwhile, restraint stress partially increased ethanol intake ($P < 0.01$; Fig. 1C). Sucrose preference was significantly reduced by restraint stress ($P < 0.05$), but it was not reduced by IS (Fig. 1D).

Ethanol CPP during IS

From the conditioned place preference (CPP) test, an increased ethanol place preference was observed in mice subjected to IS. The ethanol place preference score in the reinstatement test following extinction (for 8 days) was significantly elevated in the IS group compared to both the control and saline-injected groups ($P < 0.01$ and $P < 0.05$, respectively; fig. S2E).

Changes in body weight and food intake

The mice gained approximately 2 g of body weight after 4 weeks, and changes in body weight among the groups were not affected by IS and/or ethanol intake (fig. S2A). During the experimental days, food intake tended to decrease in mice subjected to IS along with ethanol but was not significantly different among the four groups (fig. S2B).

[1]Institute of Bioscience & Integrative Medicine, Dunsan Hospital of Daejeon University, Daejeon, Republic of Korea. [2]Department of Anatomy, Brain Research Institute, Chungnam National University School of Medicine, Daejeon, Republic of Korea. [3]Department of Physiology, College of Korean Medicine, Daegu Haany University, Daegu, Republic of Korea.
*Corresponding author. Email: ckson@dju.ac.kr

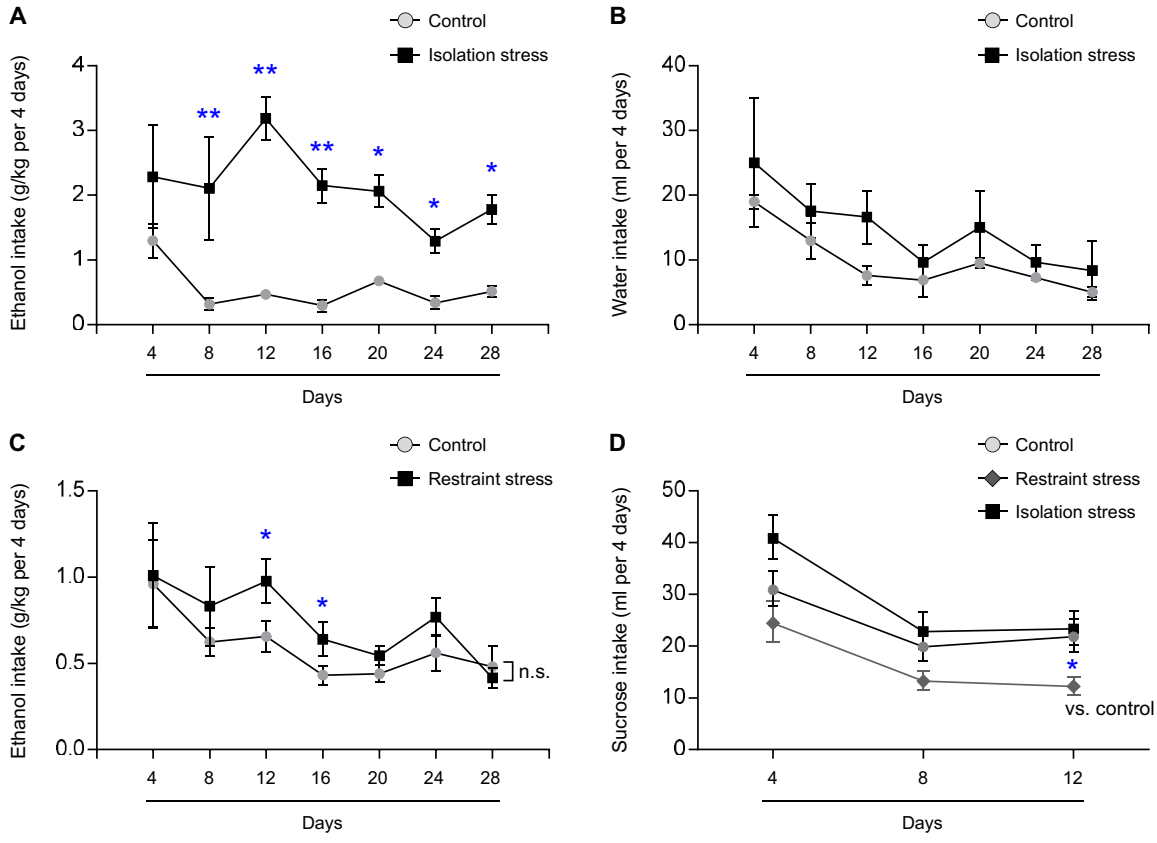

Fig. 1. Ethanol intake in mice exposed to control and IS conditions. To evaluate ethanol preference under unstressed and IS conditions, ethanol (**A**) and water (**B**) intake were monitored for 28 days. In addition, ethanol intake (**C**) in mice subjected to restraint stress and sucrose intake (**D**) during restraint stress or IS were recorded for 28 and 12 days, respectively. The data are expressed as the means ± SD ($n = 8$). *$P < 0.05$ and **$P < 0.01$ compared to the unstressed mice. n.s., not significant.

Changes in serum ethanol concentrations and serum levels of aspartate transaminase and alanine transaminase

Serum ethanol concentrations were significantly increased by ethanol intake, irrespective of whether mice were subjected to IS ($P < 0.05$ for both) or not (fig. S2G). Serum aspartate transaminase (AST) and alanine transaminase (ALT) levels were not altered by IS and/or voluntary ethanol intake (fig. S2, H and I).

Changes in anxiety- and depressive-like behaviors

In the open field test (OFT; total distance traveled and time spent in the center) and elevated plus maze (EPM; distance traveled, number of arm entries, number of open arm entries, and time spent time in the open arms), IS significantly induced anxiety-like behaviors ($P < 0.05$ or $P < 0.01$) compared to those in the respective control groups. These alterations following IS were remarkably exacerbated by ethanol intake ($P < 0.05$ and $P = 0.071$; Fig. 2A, a and b; $P < 0.05$ for all parameters; Fig. 2B, a to d).

The results from both the forced swimming test (FST; total global activity, immobility duration, and activity duration) and tail suspension test (TST; total global activity, immobility duration, and latency to immobility) indicated that IS induced a considerable increase in depressive-like behaviors ($P < 0.05$ or $P < 0.01$) compared to those in the respective control groups. In particular, depressive-like behaviors were most intense in mice that both were exposed to IS and had assess to ethanol ($P < 0.05$ and $P = 0.081$, respectively; Fig. 2C, a and b; $P < 0.05$ for all parameters; Fig. 2D, a to c). In contrast, the mice receiving a single injection of ethanol (1 g/kg, intraperitoneally) at night (02:00 hours, main active hour) showed a slight alleviation of depressive-like behaviors, as shown in the FST 12 hours later at 14:00 hours ($P < 0.05$; fig. S2C).

Changes in serotonergic signals and microglial activity

Serotonergic activity in the raphe nuclei (dorsal and median) was prominently inhibited by IS, as shown by both 5-hydroxytryptamine (5-HT; $P < 0.01$) and tryptophan hydroxylase 2 (TPH2; $P < 0.01$) staining, compared to that in control conditions (Fig. 3 and fig. S3) but not by ethanol intake alone. These two suppressed signals were further emphasized in the dorsal raphe nuclei of mice subjected to IS along with ethanol ($P < 0.05$ for both; Fig. 3, A and B, and fig. S3, A to D).

In contrast to serotonergic activity, activation of microglia, as evaluated by increases in the intensity, numbers, and soma area of the Iba-1–positive cells in the dorsal raphe nucleus, was greater in the IS group than in the respective control groups ($P < 0.05$ or $P < 0.01$; Fig. 3, A and C to E). Moreover, microglial activation was further increased by ethanol intake ($P < 0.05$ or $P < 0.01$; Fig. 3, A and C to E). This phenomenon was also observed by immunohistochemical staining with Iba-1 ($P < 0.01$; fig. S3, E and F).

Changes in microglial function and inflammatory cytokine

IS significantly increased microglial activation (Iba-1) and phagocytosis-derived molecules involved in synaptic pruning (C1q and cleaved

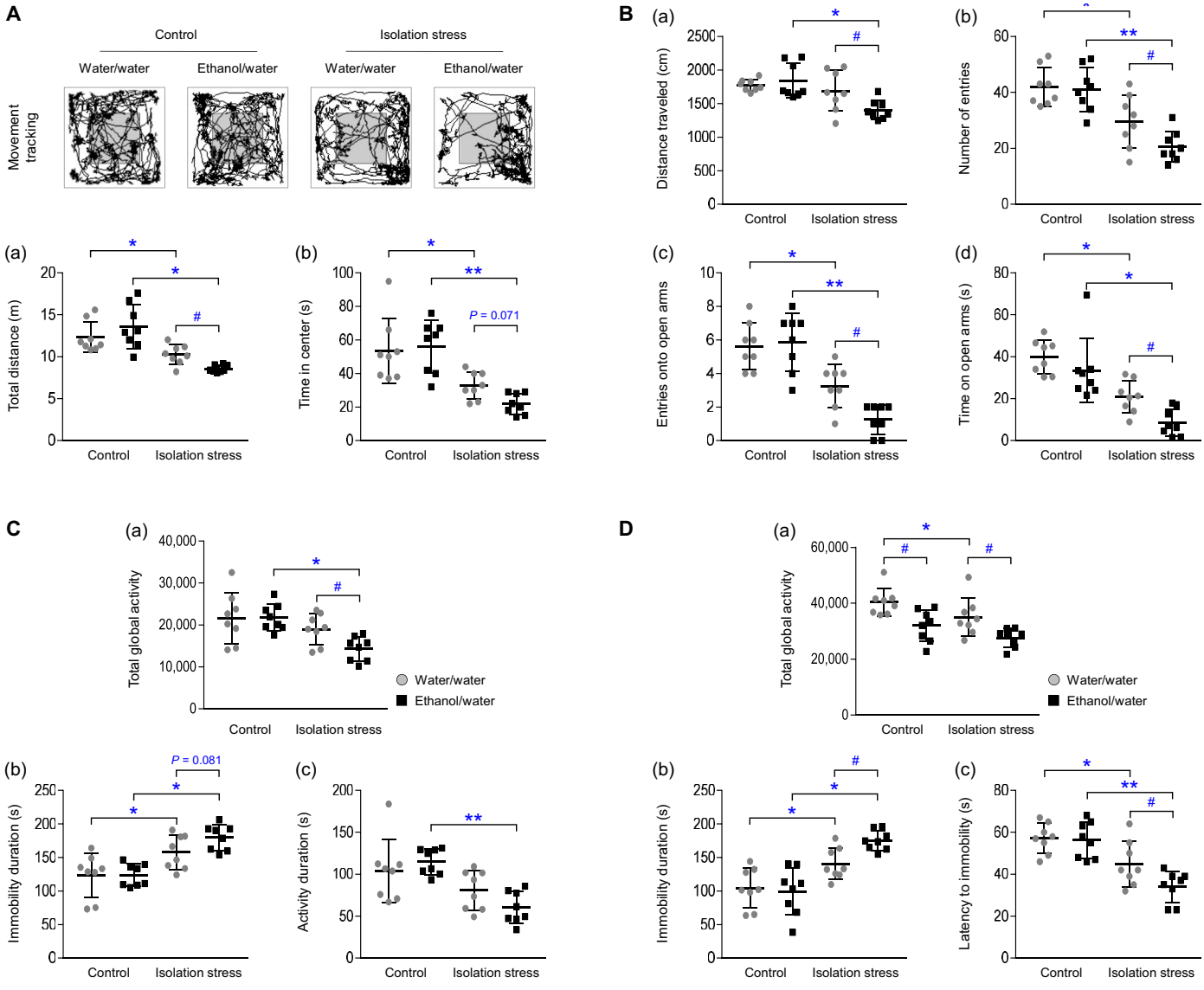

Fig. 2. Depressive- and anxiety-like behaviors. After IS with or without ethanol exposure, the total distance traveled (a) and time spent in the center (b) in the OFT (**A**) were assessed on the 28th day. After a period of 6 hours, total global activity (a), immobility duration (b), and activity duration (c) in the TST (**C**) were assessed. The traveled distance (a), total number of entries (b), entries into the open arms (c), and spent time in the open arms (d) in the EPM (**B**) were assessed on the 29th day. Total global activity (a), immobility duration (b), and latency to immobility (c) in the FST (**D**) were assessed on the 30th day. The data are expressed as the means ± SD ($n = 8$). *$P < 0.05$ and **$P < 0.01$ compared to the unstressed mice, and #$P < 0.05$ compared to the mice not exposed to ethanol.

caspase 3) in the raphe nuclei ($P < 0.05$ or $P < 0.01$; Fig. 4A and B). In contrast, the levels of postsynaptic density protein (PSD) 95 and synaptophysin were notably reduced in the group of mice exposed to IS ($P < 0.05$ or $P < 0.01$; Fig. 4, A and B) compared to those in the respective control groups. IS-derived alterations were further enhanced by voluntary ethanol intake ($P < 0.05$ for both Iba-1 and synaptophysin and $P < 0.01$ for both C1q and cleaved caspase 3; Fig. 4, A and B).

Accordingly, microglia-mediated neuroinflammation was triggered by IS in the raphe nuclei, as evidenced by differences in the levels of proinflammatory cytokines (tumor necrosis factor, TNF-α) and anti-inflammatory cytokines (interleukin, IL-10) compared to those in the respective control groups ($P < 0.05$ for both parameters; Fig. 4, C and D). These neuroinflammatory responses were noticeably further enhanced by exposure to ethanol intake ($P < 0.01$ for both parameters; Fig. 4, C and D). To confirm whether ethanol directly activates microglia, BV2 cells were activated by lipopolysaccharide (LPS). The gene expression levels of TNF-α and IL-1β were significantly increased by ethanol treatment (150 mM; $P < 0.05$ and $P < 0.01$, respectively; Fig. 4, E and F). The low dose of ethanol (20 mM) also increased IL-1β mRNA levels ($P < 0.05$; fig. S2F).

Effects of a microglial inhibitor

Administration of minocycline (a selective microglial inhibitor) completely prevented microglial-mediated loss of the serotonergic indicators (Fig. 5, A and B). Minocycline also alleviated the IS-induced overactivation of microglia (Fig. 5, C and D), which was supported by differences in C1q protein and C1qa mRNA levels ($P < 0.05$;

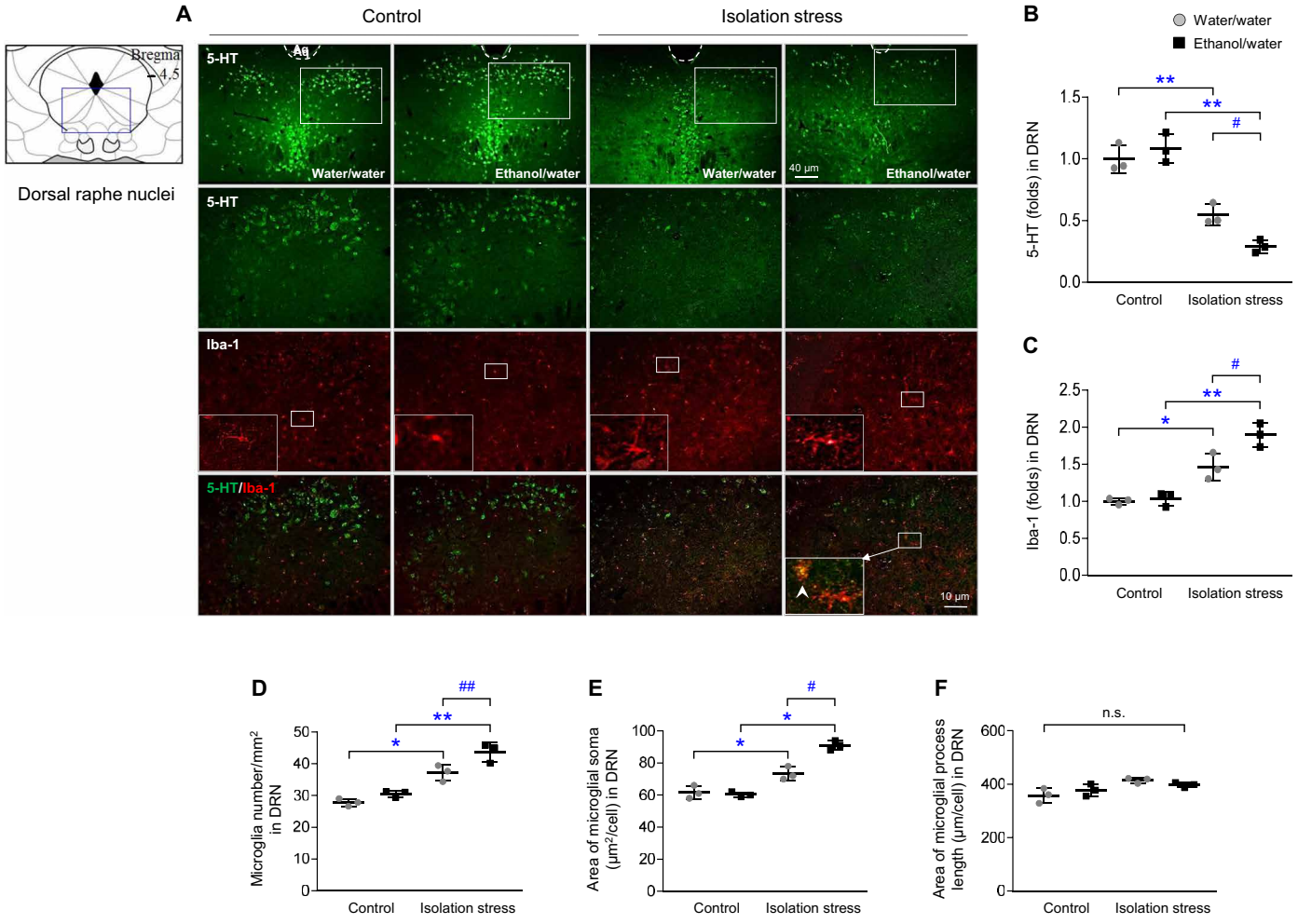

Fig. 3. Serotonergic signals and microglial activation. After IS with or without ethanol exposure for 28 days, mice were euthanized by transcardial perfusion. Serotonergic and microglial activity was assessed by immunofluorescence analysis of 5-HT and Iba-1 (**A**) in the dorsal raphe nuclei (DRN), and their intensities were semiquantified (**B** and **C**). Microglial cell numbers (**D**), soma area (**E**), and length (**F**) were quantified. The data are expressed as the means ± SD ($n = 3$). *$P < 0.05$ and **$P < 0.01$ compared to the unstressed mice, and #$P < 0.05$ and ##$P < 0.01$ compared to the mice not exposed to ethanol.

Fig. 5E). Moreover, minocycline significantly improved depressive-like behaviors, as shown in the FST, including immobility duration and latency to immobility ($P < 0.05$ and $P < 0.01$, respectively; Fig. 5, F and G).

Changes in the mesolimbic dopaminergic system

In the mice exposed to a socially isolated environment, there were increases in both tyrosine hydroxylase (TH; $P < 0.01$) and dopamine ($P < 0.01$) levels in the ventral tegmental area (VTA). These two signals were markedly higher in mice subjected to IS and ethanol than in mice subjected to stress only ($P < 0.05$ and $P < 0.01$, respectively; Fig. 6, A to C). Significant increases in the dopaminergic projections into the nucleus accumbens (NAc) were shown by c-Fos translocation to the nucleus (fig. S4A).

DISCUSSION

The above results clearly demonstrated the mutual interaction between depressive-like behaviors and ethanol consumption. Although free access was given to both water and ethanol (the two-bottle choice procedure), social IS markedly induced a radical increase in ethanol intake (i.e., sixfold increase at approximately 2 weeks; Fig. 1A and movies S1 and S2). To verify ethanol-seeking behavior, we additionally assessed ethanol-induced CPP suing a tactile conditioned stimulus. The ethanol preference score (on the day of the reinstatement test) was considerably increased by IS (fig. S2E). We confirmed that ethanol consumption was much more prominent during IS conditions than in conditions involving restraint stress (Fig. 1C). The serum ethanol concentrations were significantly increased in the two groups given the choice of ethanol intake. However, there was no significant difference between the IS and the control group (assessed at approximately 14:00 hours) in blood ethanol concentration (fig. S2G), which might be explained by the rapid metabolism; ethanol in the C57BL/6J mouse is metabolized within 5 hours in the blood (*23*). Among the groups, metabolism rates may not be different because the liver was intact (fig. S2, H and I). An additional experiment confirmed that ethanol overconsumption was exhibited by female mice (fig. S2D).

Notably, IS-induced depressive-like and anxiety-related behaviors were aggravated by ethanol consumption, as we expected

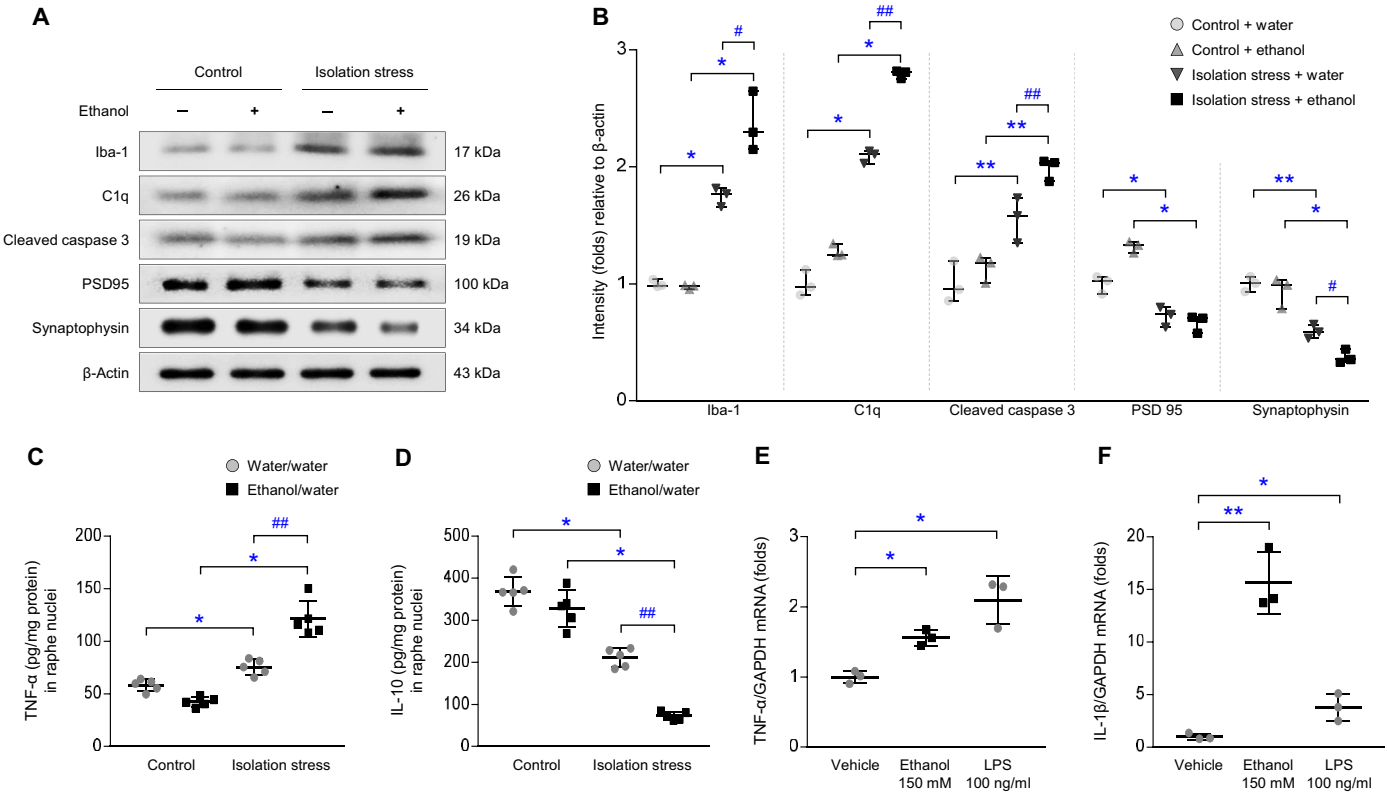

Fig. 4. Microglia synaptic pruning and neuroinflammation. After IS with or without ethanol exposure for 28 days, mice were euthanized. Raphe nuclei homogenates were used to analyze protein and cytokine expression. The protein levels of Iba-1, PSD95, synaptophysin, cleaved caspase 3, and C1q were determined by Western blotting (**A**), and their intensities were semiquantified (**B**). Levels of the cytokines TNF-α (**C**) and IL-10 (**D**) in the raphe nuclei were determined by enzyme immunoassay. The data are expressed as the means ± SD ($n = 5$). *$P < 0.05$ and **$P < 0.01$ compared to the unstressed mice, and #$P < 0.05$ and ##$P < 0.01$ compared to the mice not exposed to ethanol. Gene expression levels of TNF-α (**E**) and IL-1β (**F**) were determined by real-time PCR analysis. The data are expressed as the means ± SD ($n = 3$). *$P < 0.05$ and **$P < 0.01$ compared to the vehicle-treated cells.

(Fig. 2, A to D). We verified that these behavioral changes were not induced by acute ethanol exposure (fig. S2C). Previous animal studies using IS models, such as maternal separation or adolescent social isolation, have shown a similar pattern of ethanol craving (*24*–*26*). Poor relationships with friends or family members are considered to be a factor underlying the co-occurrence of both depression and AUD (*27*), and their comorbidity is a significant concern worldwide (*28*). Heavy or frequent drinking increases the risk of depressive symptoms during adolescence (twofold higher than in adulthood) (*29*). Under the current COVID-19 pandemic crisis condition, clinical studies have revealed a positive association between social isolation and increases in depressive disorder and alcohol misuse (*7*, *30*, *31*). However, the mechanisms underlying this interaction remain unclear.

To explain the interactive mechanisms, we examined relevant neurotransmitter systems and related mediators. Sociality is regulated by serotonergic innervation from the raphe nuclei (*32*, *33*), and it plays a pivotal role in coping with inescapable stress (*34*). Serotonin depletion is a common feature of the pathophysiology of MDD (*35*, *36*), and a previous meta-analysis found a functional genetic variant of TPH2 (a rate-limiting enzyme in the synthesis of 5-HT) in patients with major depression (*37*). As we expected, social IS conspicuously reduced 5-HT (serotonin) and TPH2 signals in the raphe nuclei. Moreover, this hyposerotonergic activity was significantly exacerbated by ethanol intake (Fig. 3 and fig. S3). The alcohol-mediated disruption of the serotonergic system has been indicated in both clinical- and animal-based data: 5-HT depletion has been observed in the cerebrospinal fluid of those with AUD and in the raphe nuclei of adolescent rats exposed to ethanol binge (*38*, *39*). We thus speculate that social isolation–derived serotonergic depletion causes depressive-like behaviors and sequentially leads to ethanol-seeking and vice versa.

Drinking habits are an obstacle in the course of treatment for depressive disorders in clinics, which leads to a reduced response, up to 70%, to SSRIs (*40*). Recently, microglia have emerged as a promising target for the treatment of depression (*41*, *42*). A positron emission tomography (PET) imaging study found microglial activation in patients with depression (*43*). An animal study evidenced microglial hyperactivity lasting for more than 30 days after 4-day binge alcohol exposure (*44*). In our results, concomitant IS and ethanol intake activated microglia around serotonergic neuronal cells in the dorsal raphe nucleus in an additive manner (Fig. 3). These results might be supported by other data showing the connection between microglial activation and 5-HT neuronal inactivity (*45*, *46*). Microglia have emerged as important players in the synapse pruning process in both developing and aging brains (*47*–*49*), and their by-product C1q, microglial-derived complement cascade protein, induces neuronal cell death (*50*). Positive correlations between high serum C1q levels and the severity of depression were observed in patients with MDD (*51*). As expected, IS and ethanol

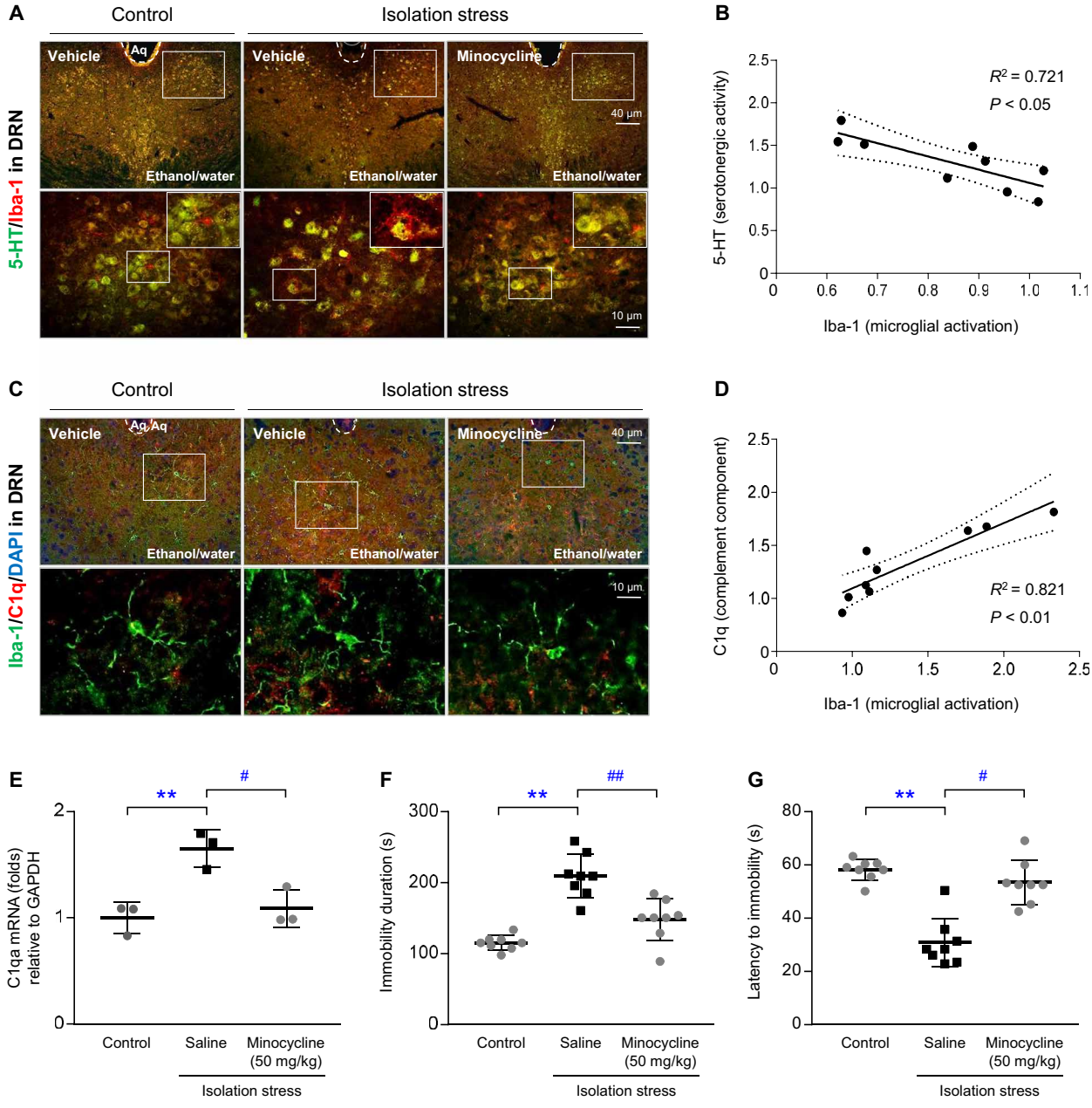

Fig. 5. Effects of minocycline on serotonergic depletion, microglial activation, ethanol intake, and depressive-like behavior. Following IS with ethanol exposure and minocycline injection for 28 days, the mice were euthanized. Microglial-derived serotonergic depletion was confirmed by immunofluorescence analysis of 5-HT and Iba-1 (**A**), and microglial activity was assessed by costaining of Iba-1 and C1q (**C**) in the dorsal raphe nuclei. Simple linear regression analyses were performed (**B** and **D**). Raphe nuclei homogenates were used to analyze C1q gene expression (**E**). In another experiment, ethanol intake (**F**) was assessed, and depressive-like behavior was assessed using the FST (**G**). The data are expressed as the means ± SD ($n = 3$ or 8). $^{**}P < 0.01$ compared to the unstressed mice, and $\#P < 0.05$ and $\#\#P < 0.01$ compared to the mice not injected with minocycline. DAPI, 4′,6-diamidino-2-phenylindole; GAPDH, glyceraldehyde-3-phosphate dehydrogenase.

consumption led to considerable synaptic loss, as evidenced by the increased levels of Iba-1, C1q, and cleaved caspase 3, but decreases in synaptophysin and PSD95 (indicators of pre- and postsynaptic activity, respectively) in the raphe nuclei (Fig. 4, A and B).

Regarding the involvement of microglia in alcohol-related behaviors and molecular alterations, we conducted a confirmatory experiment using minocycline, a selective inhibitor of microglial activation. Minocycline has pharmacological properties against several neurological disorders by inhibiting microglial activation and neuroinflammation-related molecules, such as caspase-1–dependent IL-1β and inducible nitric oxide (*52*). As expected, treatment with minocycline significantly attenuated microglial hyperactivation, synaptic pruning, and depressive-like behaviors (Fig. 5). A double-blind randomized clinical trial revealed the therapeutic potential of minocycline in patients with MDD tolerant to commonly used antidepressant (*53*). These results indicated the pathogenetic roles of microglial hyperactivation in serotonergic damage in IS and ethanol overconsumption conditions. On the other hand, scientists well

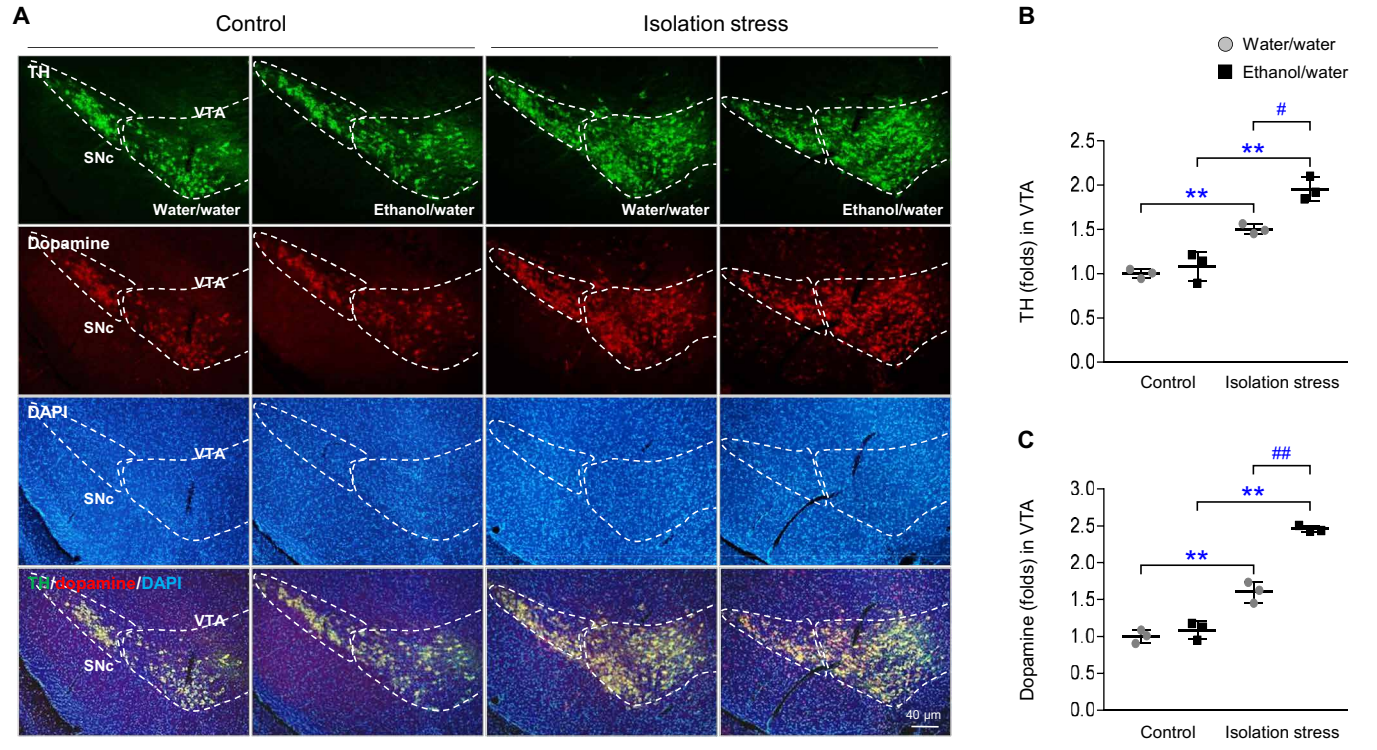

Fig. 6. Dopaminergic reward system. After IS with or without ethanol exposure for 28 days, mice were euthanized by transcardial perfusion. Dopaminergic signals were assessed by immunofluorescence analysis of TH and dopamine in the VTA (**A**), and their signals were semiquantified (**B** and **C**). SNc, substantia nigra pars compacta. The data are expressed as the means ± SD ($n = 3$). $^{**}P < 0.01$ compared to the unstressed mice, and $\#P < 0.05$ and $\#\#P < 0.01$ compared to the mice not exposed to ethanol.

noticed the vital functions of activated microglia-derived proinflammatory cytokines in the poor sociality and depressive-like behavior (*54*, *55*). Our data revealed the IS-derived alterations in TNF-α and IL-10 levels in the brain and exacerbation by exposure to ethanol (Fig. 4, C and D). Ethanol directly increased TNF-α and IL-1β gene expression in a BV2 microglial cell line (Fig. 4, E and F).

We further investigated the mechanisms underlying ethanol craving from the perspective of the reward system. Dysregulated reward circuitry is common among patients with substance (nicotine and alcohol) use disorders and neuropsychiatric disorders including depression or anxiety (*56*). Compared to artificial stimuli such as restraint or foot shock stress, social defeat–like stress is known to sensitize rodents to ethanol- or cocaine-related rewards (*57*). In our study, the mice that were exposed to restraint stress did not exhibit a strong response to ethanol (Fig. 1C), while IS markedly increased both TH and dopamine signals in the VTA region; this effect of IS was significantly facilitated by ethanol consumption (Fig. 6, A to C). Moreover, IS produced changes in neuronal firing (c-Fos–positive activity) in NAc, although changes in the dopaminergic project from VTA were uncertain (fig. S4). One group observed higher activity of dopaminergic reward circuits in patients with social anxiety disorder than in healthy controls using functional magnetic resonance imaging analysis (*58*).

Although we conducted a comprehensive experiment, there are some limitations, for example, adoption of only a single animal model and one age group (6-week-old mice). Compared with adult rodents, young rodents are known to be more susceptible to voluntary ethanol consumption during IS conditions (*51*). Although each variable (social isolation, ethanol, and neuroinflammation) is known as a risk factor, the novel findings from this study are as follows: (i) Our findings provide the first evidence to verify the interconnections among these factors, especially regarding the vicious cycle of the relationship; (ii) we are the first to provide these novel mechanistic insights into the causative role of microglia in clinical comorbidity between depressive disorders and AUDs, as summarized in fig. S5; and (iii) these are interesting findings that verify the mutual specificity of IS (not restraint stress) and ethanol (not sucrose), respectively. Our findings provide insight and ideas to physicians and scientists to develop a therapeutic strategy for the growing number of depressed patients living in solitary environments and their alcohol issues.

MATERIALS AND METHODS

Animal and experimental design

Specific pathogen–free male adolescent C57BL/6J mice (5 weeks old, 21 to 23 g) were purchased from Dae Han Bio Link Co. Ltd. (Eumseong, Republic of Korea). They were maintained under a thermo hygrostat (temperature: 23° ± 2°C and humidity: 55 ± 10%; ALFFIZ, Busung Co. Ltd., Seoul, Republic of Korea) on a 12-hour light-dark cycle (09:00 to 21:00 hours), freely fed food pellets (Cargill Agri Purina, Gyeonggi-do, Republic of Korea), and provided two bottles of tap water before the experiments began. For all experiments, the mice, except those in the control groups (three to five mice per cage), were individually housed for 28 days to induce a depressive-like state. Voluntary ethanol intake, food intake, and body weight were recorded over these 28 days (twice per week).

Three main studies were conducted as described below. After acclimation for 1 week, the mice were randomly divided into the following three experiments ($n = 32$ per experiment): Experiment 1,

which was performed to assess ethanol-related behaviors and depressive- and anxiety-like behaviors; experiment 2, which was performed to analyze cytokine and immunohistological alterations; and experiment 3, which was performed to determine serum biochemical and protein alterations. The mice in each experiment were divided into the following four groups (n = 8 per group) based on two variables, namely, social IS and voluntary ethanol intake: control with two bottles of tap water, control with both tap water and 10% ethanol, IS with two bottles of tap water, and IS with both tap water and 10% ethanol. During the 1-week acclimation period, the mice were adapted to the two-bottle choice procedure (two bottles containing tap water). To achieve a human-like approach to drinking, mice were allowed to spontaneously consume tap water and/or 10% ethanol for 28 days, with the positioning of the two bottles being changed at 4-day intervals.

To conduct six additional studies, the experiments were designed as follows: experiment 4, which was performed to evaluate the influence of minocycline (n = 3 or 8 per group)—control group (tap water and 10% ethanol), IS group (tap water and 10% ethanol), and IS group (tap water and 10% ethanol) receiving minocycline (50 mg/kg, intraperitoneally; daily for 28 days); experiment 5, which was performed to verify specificity of IS effects (n = 5 per group)—control group (tap water and 10% ethanol) and group (tap water and 10% ethanol) exposed to restraint stress as previously described (3 hours per day for 28 days); experiment 6, which was performed to determine specificity of ethanol effects (n = 5 per group)—control group (tap water and 1% sucrose) and social IS group (tap water and 1% sucrose); experiment 7, which was performed in female mice (n = 3 per group)—control group (tap water and 10% ethanol) and IS group (tap water and 10% ethanol); experiment 8, which was performed to confirm ethanol-seeking behaviors (n = 10 per group); and experiment 9, which was to investigate acute ethanol effects on behavioral alterations (n = 6/group). All experiments were repeated two to three times with the indicated numbers of mice. The experimental designs are displayed in fig. S1. All of the experiments were approved by the Institutional Animal Care and Use Committee of Daejeon University (DJUARB2016-037) and were conducted in accordance with the *Guide for the Care and Use of Laboratory Animals*, published by the National Institutes of Health (NIH).

Social IS protocol

The social IS procedure was performed as described previously (*59*). Briefly, the mice were individually housed in a single cage with a screen blocking visual communication for 28 days. During the period of isolation, the mice were exposed to minimal handling and were provided no environmental enrichment.

Two-bottle drinking procedure

The mice were subjected to a two-bottle choice procedure as previously described (*60*). The mice were given continuous access to either two bottles of tap water or a bottle of tap water and a bottle of 10% ethanol (v/v) in each experiment. The positioning of the two bottles (left and right) was changed at 4-day intervals to avoid the effect of preferences for a particular side, and intake was recorded.

Behavioral monitoring (experiment 1)

Open field test

Anxiety-like behavior of the mice was first tested in a large square chamber (30-cm height × 40-cm length × 40-cm width). To assess activity, the open field arena was equally divided into quadrants (20 × 20 cm), and a video camera was mounted overhead. The mice were allowed to freely explore the test arena for 5 min. After each test, the apparatus was cleaned with acetic acid (2%) to limit mouse odors. The total horizontal distance (meters) and the time spent in the center (seconds) were recorded at 50 lux illuminations on the 28th day.

Tail suspension test

Depressive-like behavior was measured using a rectangular compartment (55-cm height × 15-cm width × 12-cm depth) with an aluminum suspension bar (1 × 1 cm; positioned on the top of the box). Mouse tails were fastened with tape to the suspension bar, and the suspended mice were observed for 5 min. Level of immobility was determined on the basis of the designated thresholds for immobility duration (immobile: 0 to 120, active: 121 to 300). Total global activity, immobility, and activity durations (seconds) were recorded at 25 lux illuminations on the 28th day.

Elevated plus maze test

The mice were subjected to another assessment of anxiety-like behavior. The apparatus consisted of two opposing open arms (30-cm arm length × 5-cm arm width at 20 lux) and two closed arms (30-cm arm length × 5-cm arm width × 15-cm high walls at 90 lux) extending from a central area (5 × 5 cm) and elevated above the ground (20 cm). Each mouse was placed in the central area of the maze with access to all arms and was allowed to freely explore the maze for 5 min. The total distance traveled (centimeters), number of entries into the open arms, and time spent in the open arms were recorded on the 29th day.

Forced swimming test

The mice were subjected to the FST to measure despair-related behavior. The apparatus consisted of a plastic cylinder (30-cm height × 20-cm diameter) filled with water to 10 cm from the top at 24° ± 1°C. Each mouse was allowed to freely swim for 5 min. Level of immobility was determined on the basis of the designated thresholds for immobility duration (immobile: 0 to 120, active: 121 to 300) established by the Smart global activity module. Total global activity, immobility duration, and latency to immobility (seconds) were recorded at 30 lux illuminations on the 30th day.

Conditioned place preference

To confirm ethanol-seeking behaviors, the CPP test was adopted. The apparatus (MED-CPP-3013-2, Med Associates, VT, USA) consisted of two compartments (17.4-cm height × 12.7-cm length × 12.7-cm width at 10 lux) with a guillotine door separating the compartments. Infrared beams detected the movement of each mouse in the black (grid floor) and white (hole floor) compartments. During the preconditioning test, mice exhibiting an unconditioned preference (more than 800 s on either side) for either compartment were excluded. The ethanol-CPP paradigm was performed as follows: (i) The mice were allowed to freely explore the compartments for 20 min (preconditioning test on the first day). From the next day to the ninth day after preconditioning habituation, each mouse was confined to the respective compartment with discriminable tactile cues (grid or hole floor) for 5 min following 10 min after injection of saline or ethanol (2 g/kg, intraperitoneally). (ii) The time each mouse spent in each compartments was recorded for 20 min (post-conditioning test at 10th day). (iii) On the seventh day after extinction session, the mice were tested for 20 min immediately following saline or ethanol (1 g/kg, intraperitoneally) injection (reinstatement test at 18th day). The following formula was used to calculate the

data: Preference score = [time spent in ethanol-induced CPP – time spent in another side].

All behavioral tests were performed in the light phase between 13:00 and 17:00 hours after habituation in the testing environments for 30 min. Tracking data from the recorded behavioral sessions were calculated using video from a video camera connected to corresponding software (SMART 3.0, Panlab SL, Barcelona, Spain or EthoVision XT, Noldus IT, Wageningen, The Netherlands). Behavioral tests were performed by researchers blinded to the experimental conditions.

Sample preparation (experiment 2)

The day after the last day of IS, the mice were euthanized under CO_2 anesthesia conducted in the daytime (13:00 to 17:00 hours). Serum was collected from abdominal blood by centrifugation at 3000*g* for 15 min. The brains of five mice from each group were immediately removed. Brain regions were isolated using a coronal mouse brain matrix (1 mm; BSMAS001-1, Zivic Instruments) and biopsy punch (1 mm; BP-10F, Kai Medical). For biochemical analysis, samples were homogenized in radioimmunoprecipitation assay buffer (R0278, Sigma-Aldrich) supplemented with protease inhibitors (no. 11836153001, Roche). The total protein concentration was measured using a bicinchoninic acid protein assay kit (BCA1 and B9643, Sigma-Aldrich). The absorbance was measured using an ultraviolet (UV) spectrophotometer at 562 nm (Molecular Devices Corp., Sunnyvale, CA, USA). For immunohistological analyses, the three remaining mice from each group were transcardially perfused with 0.05% heparin [10 U/ml in phosphate-buffered saline (PBS)] followed by 4% paraformaldehyde (pH 6.9). The brains were placed in the same solution for fixation.

Immunofluorescence analysis

Immunofluorescence staining was performed to assess microglial activity (Iba-1), serotonergic activity (5-HT and TPH2) in the raphe nuclei, dopaminergic activity (TH and dopamine) in the VTA, and neural activity (c-Fos) in the NAc. The brains were gradually cryoprotected in 10, 20, and 30% sucrose for 24 hours each and were subsequently embedded in optimal cutting temperature compound (Leica Microsystems, Bensheim, Germany) in liquid nitrogen. They were cut into frozen coronal sections (35 μm) using a cryostat (CM3050_S, Leica). The sections were stored free floating in buffer. After washing with ice-cold PBS, parallel free-floating sections were treated with blocking buffer (5% normal chicken serum in PBS and 0.3% Triton X-100 for 1 hour at 4°C) and incubated with anti-rabbit Iba-1 polyclonal (1:400; no. 019-19741, Wako Biologicals), anti-rat C1q monoclonal (1:10; ab11861, Abcam), anti-goat 5-HT polyclonal (1:200; ab66047, Abcam), anti-rabbit TPH2 polyclonal (1:500; NB100-74555, Novus), anti-rabbit TH polyclonal (1:500; NB300-109, Novus), anti-mouse dopamine monoclonal (1:500; NB110-2538, Novus), and anti-rabbit c-Fos polyclonal (1:100; NBP1-74555, Novus) primary antibodies overnight at 4°C. After washing with ice-cold PBS, the sections were incubated with a donkey anti-goat immunoglobulin G (IgG) H&L (1:400; Alexa Fluor 488, ab150129), goat anti-rabbit IgG H&L (1:400; Alexa Fluor 488, ab150077), goat anti-mouse IgG H&L (1:400; Alexa Fluor 488, ab150113), goat anti-rabbit IgG H&L (1:400; Alexa Fluor 594, ab150080), goat anti-mouse (1:400; Alexa Fluor 594, ab150116), or goat anti-rat (1:400; Alexa Fluor 594, ab150160) secondary antibodies for 2 hours at 4°C. The sections were subsequently exposed to 4′,6-diamidino-2-phenylindole (1:1000; D9542, Sigma-Aldrich) to stain the cell nuclei.

Immunohistochemical analysis of Iba-1 (microglial activity) was performed in the dorsal raphe nucleus. The sections were incubated with a primary antibody against Iba-1 (1:200; no. 019-19741, Wako Biologicals) overnight at 4°C. The sections were incubated with a horseradish peroxidase (HRP)–conjugated goat anti-rabbit IgG (1:400; ab6722, Abcam) secondary antibody for 2 hours at room temperature. For amplification of the signal, the sections were exposed to an avidin-biotin peroxidase complex (Vectastain ABC kit, Vector Laboratories) for 2 hours. Peroxidase activity was visualized using stable diaminobenzidine solution. Immunoreactivity was observed under an AxioPhot microscope (Carl Zeiss, Germany). Signals were quantified using ImageJ 1.46 software (NIH, Bethesda, MD, USA), and morphological characteristics of stained microglia (average cell body size per cell, average dendritic process per cell, and cell number per mm^2) were analyzed by using image analysis software (Image-Pro Plus 6.0, Media Cybernetics Inc., Rockville, USA).

Western blot analysis

The protein expression levels of Iba-1, C1q, cleaved caspase 3, synaptophysin, PSD95, and β-actin in raphe nuclei homogenates were evaluated using Western blotting. The protein concentrations of the homogenates were equalized, and the samples were separated by 10% polyacrylamide gel electrophoresis and transferred to polyvinylidene fluoride membranes. To minimize nonspecific binding, the membranes were blocked in 5% bovine serum albumin for 1 hour. The membranes were incubated overnight at 4°C with the following primary antibodies: Iba-1 (1:500; 061-20001, Wako Biologicals), C1q (1:50; ab71940, Abcam), cleaved caspase 3 (1:200; no. 9664S, Cell Signaling Technology), PSD95 (1:200; ab13552, Abcam), synaptophysin (1:500; ab8049, Abcam), or β-actin (1:2500; PA1-183, Thermo Fisher Scientific). After washing, the membranes were incubated with an HRP-conjugated anti-rabbit or anti-mouse antibody (GeneTex Inc., Irvine, CA) for 1 hour. The Western blotting results were visualized with an enhanced chemiluminescence advanced kit. The intensity was analyzed by ImageJ version 1.46 (NIH, Bethesda, MD, USA).

Pro- and anti-inflammatory cytokines

TNF-α and IL-10 levels in raphe nuclei homogenates were determined using commercially available enzyme immunoassay (OptEIA) kits for TNF-α (no. 558534, BD Biosciences, San Diego, CA, USA) and IL-10 (no. 555252, BD Biosciences, San Diego, CA, USA), and the absorbance was measured at 450 and 570 nm using a UV spectrophotometer (Molecular Devices Corp., Sunnyvale, CA, USA).

Ethanol concentrations

The serum levels of ethanol (K610, BioVision, Milpitas, CA, USA) were measured using an ethanol colorimetric assay kit. Absorbance was measured at 450 or 570 nm using a UV spectrophotometer (Molecular Devices Corp., Sunnyvale, CA, USA).

AST and ALT levels

The serum levels of AST and ALT were determined using an autoanalyzer (Chiron Diagnostics Co.).

Real-time quantitative polymerase chain reaction (in vitro experiment)

Mouse microglial cells (BV2 cells) were cultured in Dulbecco's modified Eagle's medium (DMEM) supplemented with 10% fetal bovine serum and 1% penicillin-streptomycin. BV2 cells were incubated at

37°C under 5% CO_2. BV2 cells were seeded into six-well plates at a density of 2×10^5 cells per well. After incubation for 12 hours, the BV2 cells were treated with PBS or LPS (100 ng/ml) from *Escherichia coli* O111:B4 (no. L2630, Sigma-Aldrich) or 10, 20, or 150 mM ethanol for 24 hours. Ethanol-treated cells were incubated under a beaker containing 200 ml of 4% ethanol to prevent the evaporation of ethanol from the media. To confirm whether ethanol induces microglial activation, the gene expression of inflammatory cytokines was measured in cell lysates.

The mRNA expression of genes encoding TNF-α, IL-1β, and glyceraldehyde-3-phosphate dehydrogenase in BV2 cells or C1qa in raphe nuclei homogenates from mice was measured by real-time polymerase chain reaction (PCR). Total mRNA was extracted using an RNeasy Mini Kit (QIAGEN, Valencia, CA, USA), and cDNA was synthesized using a High-Capacity cDNA Reverse Transcription Kit (Ambion, Austin, TX, USA). Real-time PCR was performed using SYBR Green PCR Master Mix (Applied Biosystems, Foster City, CA, USA), and PCR amplification was performed using a standard protocol on an IQ5 PCR Thermal Cycler (Bio-Rad, Hercules, CA, USA). Information regarding the primer sequences is summarized in table S1.

Statistical analysis

All results are expressed as the means ± SD. Statistical analysis was performed by using two-way analysis of variance (ANOVA) followed by post hoc analysis by Bonferroni *t* test with exposure (control or IS) and drink (tap water or ethanol) as the between-subject variables using IBM Statistical Package for the Social Sciences (SPSS) statistics software, ver. 25.0 (SPSS Inc., Chicago, IL, USA). Differences at $P < 0.05$ indicate statistical significance. For correlations, a linear regression analysis was performed.

SUPPLEMENTARY MATERIALS

Supplementary material for this article is available at https://science.org/doi/10.1126/sciadv.abj3400

View/request a protocol for this paper from *Bio-protocol*.

REFERENCES AND NOTES

1. M. van Winkel, N. A. Nicolson, M. Wichers, W. Viechtbauer, I. Myin-Germeys, F. Peeters, Daily life stress reactivity in remitted versus non-remitted depressed individuals. *Eur. Psychiatry* **30**, 441–447 (2015).
2. E. Isometsa, Suicidal behaviour in mood disorders–Who, when, and why? *Can. J. Psychiatry* **59**, 120–130 (2014).
3. R. H. S. van den Brink, N. Schutter, D. J. C. Hanssen, B. M. Elzinga, I. M. Rabeling-Keus, M. L. Stek, H. C. Comijs, B. Penninx, R. C. Oude Voshaar, Prognostic significance of social network, social support and loneliness for course of major depressive disorder in adulthood and old age. *Epidemiol. Psychiatr. Sci.* **27**, 266–277 (2018).
4. L. Achterbergh, A. Pitman, M. Birken, E. Pearce, H. Sno, S. Johnson, The experience of loneliness among young people with depression: A qualitative meta-synthesis of the literature. *BMC Psychiatry* **20**, 415 (2020).
5. Y. C. Shin, D. Lee, J. Seol, S. W. Lim, What kind of stress is associated with depression, anxiety and suicidal ideation in korean employees? *J. Korean Med. Sci.* **32**, 843–849 (2017).
6. K. Endo, S. Ando, S. Shimodera, S. Yamasaki, S. Usami, Y. Okazaki, T. Sasaki, M. Richards, S. Hatch, A. Nishida, Preference for solitude, social isolation, suicidal ideation, and self-harm in adolescents. *J. Adolesc. Health* **61**, 187–191 (2017).
7. D. Fancourt, A. Steptoe, F. Bu, Trajectories of anxiety and depressive symptoms during enforced isolation due to COVID-19 in England: A longitudinal observational study. *Lancet Psychiatry* **8**, 141–149 (2021).
8. J. Simard, L. Volicer, Loneliness and isolation in long-term care and the COVID-19 pandemic. *J. Am. Med. Dir. Assoc.* **21**, 966–967 (2020).
9. P. R. Albert, C. Benkelfat, L. Descarries, The neurobiology of depression—Revisiting the serotonin hypothesis. I. Cellular and molecular mechanisms. *Philos. Trans. R. Soc. Lond. B Biol. Sci.* **367**, 2378–2381 (2012).
10. F. Artigas, Serotonin receptors involved in antidepressant effects. *Pharmacol. Ther.* **137**, 119–131 (2013).
11. B. N. Gaynes, D. Warden, M. H. Trivedi, S. R. Wisniewski, M. Fava, A. J. Rush, What did STAR*D teach us? Results from a large-scale, practical, clinical trial for patients with depression. *Psychiatr. Serv.* **60**, 1439–1445 (2009).
12. P. W. Andrews, J. A. Thomson Jr., A. Amstadter, M. C. Neale, *Primum non nocere*: An evolutionary analysis of whether antidepressants do more harm than good. *Front. Psychol.* **3**, 117 (2012).
13. I. M. Berwian, H. Walter, E. Seifritz, Q. J. Huys, Predicting relapse after antidepressant withdrawal–A systematic review. *Psychol. Med.* **47**, 426–437 (2017).
14. R. Yirmiya, N. Rimmerman, R. Reshef, Depression as a microglial disease. *Trends Neurosci.* **38**, 637–658 (2015).
15. J. H. Meyer, S. Cervenka, M. J. Kim, W. C. Kreisl, I. D. Henter, R. B. Innis, Neuroinflammation in psychiatric disorders: PET imaging and promising new targets. *Lancet Psychiatry* **7**, 1064–1074 (2020).
16. V. Agosti, Predictors of alcohol dependence relapse during recurrence of major depression. *J. Addict. Dis.* **32**, 79–84 (2013).
17. D. S. Hasin, R. D. Goodwin, F. S. Stinson, B. F. Grant, Epidemiology of major depressive disorder: Results from the National Epidemiologic Survey on Alcoholism and Related Conditions. *Arch. Gen. Psychiatry* **62**, 1097–1106 (2005).
18. M. W. Kuria, D. M. Ndetei, I. S. Obot, L. I. Khasakhala, B. M. Bagaka, M. N. Mbugua, J. Kamau, The association between alcohol dependence and depression before and after treatment for alcohol dependence. *ISRN Psychiatry* **2012**, 1–6 (2012).
19. L. Sher, M. A. Oquendo, M. F. Grunebaum, A. K. Burke, Y. Y. Huang, J. J. Mann, CSF monoamine metabolites and lethality of suicide attempts in depressed patients with alcohol dependence. *Eur. Neuropsychopharmacol.* **17**, 12–15 (2007).
20. C. A. Okoro, R. D. Brewer, T. S. Naimi, D. G. Moriarty, W. H. Giles, A. H. Mokdad, Binge drinking and health-related quality of life: Do popular perceptions match reality? *Am. J. Prev. Med.* **26**, 230–233 (2004).
21. J. M. Boden, D. M. Fergusson, Alcohol and depression. *Addiction* **106**, 906–914 (2011).
22. I. Ponomarev, S. Wang, L. Zhang, R. A. Harris, R. D. Mayfield, Gene coexpression networks in human brain identify epigenetic modifications in alcohol dependence. *J. Neurosci.* **32**, 1884–1897 (2012).
23. D. J. Livy, S. E. Parnell, J. R. West, Blood ethanol concentration profiles: A comparison between rats and mice. *Alcohol* **29**, 165–171 (2003).
24. T. Advani, J. G. Hensler, W. Koek, Effect of early rearing conditions on alcohol drinking and 5-HT1A receptor function in C57BL/6J mice. *Int. J. Neuropsychopharmacol.* **10**, 595–607 (2007).
25. N. Yoneyama, J. C. Crabbe, M. M. Ford, A. Murillo, D. A. Finn, Voluntary ethanol consumption in 22 inbred mouse strains. *Alcohol* **42**, 149–160 (2008).
26. M. J. Caruso, L. R. Seemiller, T. B. Fetherston, C. N. Miller, D. E. Reiss, S. A. Cavigelli, H. M. Kamens, Adolescent social stress increases anxiety-like behavior and ethanol consumption in adult male and female C57BL/6J mice. *Sci. Rep.* **8**, 10040 (2018).
27. C. L. Salom, A. B. Kelly, R. Alati, G. M. Williams, G. C. Patton, J. W. Williams, Individual, school-related and family characteristics distinguish co-occurrence of drinking and depressive symptoms in very young adolescents. *Drug Alcohol Rev.* **35**, 387–396 (2016).
28. D. S. Hasin, B. F. Grant, Major depression in 6050 former drinkers: Association with past alcohol dependence. *Arch. Gen. Psychiatry* **59**, 794–800 (2002).
29. P. Pedrelli, B. Shapero, A. Archibald, C. Dale, Alcohol use and depression during adolescence and young adulthood: A summary and interpretation of mixed findings. *Curr. Addict. Rep.* **3**, 91–97 (2016).
30. M. S. Pollard, J. S. Tucker, H. D. Green Jr., Changes in adult alcohol use and consequences during the COVID-19 pandemic in the US. *JAMA Netw. Open* **3**, e2022942 (2020).
31. A. Capasso, A. M. Jones, S. H. Ali, J. Foreman, Y. Tozan, R. J. DiClemente, Increased alcohol use during the COVID-19 pandemic: The effect of mental health and age in a cross-sectional sample of social media users in the U.S. *Prev. Med.* **145**, 106422 (2021).
32. E. Edsinger, G. Dolen, A conserved role for serotonergic neurotransmission in mediating social behavior in octopus. *Curr. Biol.* **28**, 3136–3142.e4 (2018).
33. D. Kiser, B. Steemers, I. Branchi, J. R. Homberg, The reciprocal interaction between serotonin and social behaviour. *Neurosci. Biobehav. Rev.* **36**, 786–798 (2012).
34. N. Nishitani, K. Nagayasu, N. Asaoka, M. Yamashiro, C. Andoh, Y. Nagai, H. Kinoshita, H. Kawai, N. Shibui, B. Liu, J. Hewinson, H. Shirakawa, T. Nakagawa, H. Hashimoto, S. Kasparov, S. Kaneko, Manipulation of dorsal raphe serotonergic neurons modulates active coping to inescapable stress and anxiety-related behaviors in mice and rats. *Neuropsychopharmacology* **44**, 721–732 (2019).
35. M. Fakhoury, Revisiting the serotonin hypothesis: Implications for major depressive disorders. *Mol. Neurobiol.* **53**, 2778–2786 (2016).
36. A. L. Lopez-Figueroa, C. S. Norton, M. O. Lopez-Figueroa, D. Armellini-Dodel, S. Burke, H. Akil, J. F. Lopez, S. J. Watson, Serotonin 5-HT1A, 5-HT1B, and 5-HT2A receptor mRNA

expression in subjects with major depression, bipolar disorder, and schizophrenia. *Biol. Psychiatry* **55**, 225–233 (2004).
37. J. Gao, Z. Pan, Z. Jiao, F. Li, G. Zhao, Q. Wei, F. Pan, E. Evangelou, TPH2 gene polymorphisms and major depression–A meta-analysis. *PLOS ONE* **7**, e36721 (2012).
38. S. Mukherjee, S. K. Das, K. Vaidyanathan, D. M. Vasudevan, Consequences of alcohol consumption on neurotransmitters–An overview. *Curr. Neurovasc. Res.* **5**, 266–272 (2008).
39. R. P. Vetreno, Y. Patel, U. Patel, T. J. Walter, F. T. Crews, Adolescent intermittent ethanol reduces serotonin expression in the adult raphe nucleus and upregulates innate immune expression that is prevented by exercise. *Brain Behav. Immun.* **60**, 333–345 (2017).
40. (S033) predictive capacity of three comorbidity indices in estimating survival endpoints in women with early-stage endometrial carcinoma. *Oncology* **29**, (2015).
41. Y. Zhan, R. C. Paolicelli, F. Sforazzini, L. Weinhard, G. Bolasco, F. Pagani, A. L. Vyssotski, A. Bifone, A. Gozzi, D. Ragozzino, C. T. Gross, Deficient neuron-microglia signaling results in impaired functional brain connectivity and social behavior. *Nat. Neurosci.* **17**, 400–406 (2014).
42. S. Hellwig, S. Brioschi, S. Dieni, L. Frings, A. Masuch, T. Blank, K. Biber, Altered microglia morphology and higher resilience to stress-induced depression-like behavior in CX3CR1-deficient mice. *Brain Behav. Immun.* **55**, 126–137 (2016).
43. E. Setiawan, A. A. Wilson, R. Mizrahi, P. M. Rusjan, L. Miler, G. Rajkowska, I. Suridjan, J. L. Kennedy, P. V. Rekkas, S. Houle, J. H. Meyer, Role of translocator protein density, a marker of neuroinflammation, in the brain during major depressive episodes. *JAMA Psychiat.* **72**, 268–275 (2015).
44. J. A. McClain, S. A. Morris, M. A. Deeny, S. A. Marshall, D. M. Hayes, Z. M. Kiser, K. Nixon, Adolescent binge alcohol exposure induces long-lasting partial activation of microglia. *Brain Behav. Immun.* **25** (Suppl. 1), S120–S128 (2011).
45. S. Heinisch, L. G. Kirby, Fractalkine/CX3CL1 enhances GABA synaptic activity at serotonin neurons in the rat dorsal raphe nucleus. *Neuroscience* **164**, 1210–1223 (2009).
46. G. Krabbe, V. Matyash, U. Pannasch, L. Mamer, H. W. Boddeke, H. Kettenmann, Activation of serotonin receptors promotes microglial injury-induced motility but attenuates phagocytic activity. *Brain Behav. Immun.* **26**, 419–428 (2012).
47. A. H. Stephan, D. V. Madison, J. M. Mateos, D. A. Fraser, E. A. Lovelett, L. Coutellier, L. Kim, H. H. Tsai, E. J. Huang, D. H. Rowitch, D. S. Berns, A. J. Tenner, M. Shamloo, B. A. Barres, A dramatic increase of C1q protein in the CNS during normal aging. *J. Neurosci.* **33**, 13460–13474 (2013).
48. S. Hong, L. Dissing-Olesen, B. Stevens, New insights on the role of microglia in synaptic pruning in health and disease. *Curr. Opin. Neurobiol.* **36**, 128–134 (2016).
49. R. C. Paolicelli, G. Bolasco, F. Pagani, L. Maggi, M. Scianni, P. Panzanelli, M. Giustetto, T. A. Ferreira, E. Guiducci, L. Dumas, D. Ragozzino, C. T. Gross, Synaptic pruning by microglia is necessary for normal brain development. *Science* **333**, 1456–1458 (2011).
50. A. H. Stephan, B. A. Barres, B. Stevens, The complement system: An unexpected role in synaptic pruning during development and disease. *Annu. Rev. Neurosci.* **35**, 369–389 (2012).
51. T. J. Wukitsch, E. K. Reinhardt, S. W. Kiefer, M. E. Cain, Voluntary ethanol consumption during early social isolation and responding for ethanol in adulthood. *Alcohol* **77**, 1–10 (2019).
52. V. W. Yong, J. Wells, F. Giuliani, S. Casha, C. Power, L. M. Metz, The promise of minocycline in neurology. *Lancet Neurol.* **3**, 744–751 (2004).
53. M. A. Nettis, G. Lombardo, C. Hastings, Z. Zajkowska, N. Mariani, N. Nikkheslat, C. Worrell, D. Enache, A. McLaughlin, M. Kose, L. Sforzini, A. Bogdanova, A. Cleare, A. H. Young, C. M. Pariante, V. Mondelli, Augmentation therapy with minocycline in treatment-resistant depression patients with low-grade peripheral inflammation: Results from a double-blind randomised clinical trial. *Neuropsychopharmacology* **46**, 939–948 (2021).
54. A. H. Miller, C. L. Raison, The role of inflammation in depression: From evolutionary imperative to modern treatment target. *Nat. Rev. Immunol.* **16**, 22–34 (2016).
55. G. Singhal, B. T. Baune, Microglia: An interface between the loss of neuroplasticity and depression. *Front. Cell. Neurosci.* **11**, 270 (2017).
56. G. S. Dichter, C. A. Damiano, J. A. Allen, Reward circuitry dysfunction in psychiatric and neurodevelopmental disorders and genetic syndromes: Animal models and clinical findings. *J. Neurodev. Disord* **4**, 19 (2012).
57. B. C. Trainor, Stress responses and the mesolimbic dopamine system: Social contexts and sex differences. *Horm. Behav.* **60**, 457–469 (2011).
58. J. P. Lorberbaum, S. Kose, M. R. Johnson, G. W. Arana, L. K. Sullivan, M. B. Hamner, J. C. Ballenger, R. B. Lydiard, P. S. Brodrick, D. E. Bohning, M. S. George, Neural correlates of speech anticipatory anxiety in generalized social phobia. *Neuroreport* **15**, 2701–2705 (2004).
59. A. Ieraci, A. Mallei, M. Popoli, Social Isolation stress induces anxious-depressive-like behavior and alterations of neuroplasticity-related genes in adult male mice. *Neural Plast.* **2016**, 6212983 (2016).
60. J. K. Belknap, J. C. Crabbe, E. R. Young, Voluntary consumption of ethanol in 15 inbred mouse strains. *Psychopharmacology* **112**, 503–510 (1993).

Acknowledgments: We thank W.-Y. Kim and Y.-J. Jeon for technical assistance and helpful discussions. **Funding:** This research was supported by National Research Foundation of Korea (NRF) grants funded by the Ministry of Science, ICT and Future Planning (NRF-2018R1A6A1A03025221 and NRF- 2019R1G1A1007386). **Author contributions:** J.S.L. conceptualized the study and experimental design and wrote the paper. S.-B.L. helped with in vivo animal procedures, in vitro experiments, and data collection. D.-W.K. interpreted and analyzed the data. N.S. provided support with the materials and experimental procedures. S.-J.J. and C.-H.Y. provided support with the additional behavioral tests. C.-G.S. supervised the study. All authors critically reviewed the manuscript for important intellectual content and approved the final version of the manuscript. **Competing interests:** The authors declare that they have no competing interests. **Data and materials availability:** All data needed to evaluate the conclusions in the paper are present in the paper and/or the Supplementary Materials.

Submitted 6 May 2021
Accepted 16 September 2021
Published 5 November 2021
10.1126/sciadv.abj3400

ScienceAdvances

Social isolation–related depression accelerates ethanol intake via microglia-derived neuroinflammation

Jin-Seok LeeSung-Bae LeeDong-Woon KimNara ShinSeon-Ju JeongChae-Ha YangChang-Gue Son

Sci. Adv., 7 (45), eabj3400. • DOI: 10.1126/sciadv.abj3400

Science Advances (ISSN) is published by the American Association for the Advancement of Science. 1200 New York Avenue NW, Washington, DC 20005. The title *Science Advances* is a registered trademark of AAAS.